Significant Modulation of Variability and Projected Change in California Winter Precipitation by Extratropical Cyclone Activity

Edmund K.M. Chang[1], Cheng Zheng, Patrick Lanigan, Albert M.W. Yau
School of Marine and Atmospheric Sciences
Stony Brook University, Stony Brook, NY

J. David Neelin
Department of Atmospheric and Oceanic Sciences
University of California at Los Angeles, Los Angeles, CA

April 2015
Geophys. Res. Lett., Accepted June 2015

Abstract

Extratropical cyclones give rise to much of the precipitation over California. Observed California winter precipitation is highly correlated to a metric of extratropical cyclone activity over the Eastern Pacific. The lack of precipitation over the recent winters is coincident with consecutive winters of much below average cyclone activity. Analysis of variability in cyclone activity and California precipitation simulated by models participating in Coupled Model Intercomparison Project phase 5 indicates that most models can simulate the relationship between cyclone activity and precipitation well. Examination of projected change suggests 1) no evidence of a long-term downward trend in California-region cyclone activity within the examined scenarios; and 2) that the inter-model spread in California precipitation projection can be largely explained by the spread in the projection of extratropical cyclone activity. This highlights the need to further understand physical mechanisms for the variation in projection of cyclone activity in this region.

[1] Corresponding author: Dr. Edmund K.M. Chang, School of Marine and Atmospheric Sciences, Stony Brook University, Stony Brook, NY 11794-5000. Email: kar.chang@stonybrook.edu

1. Introduction

California receives most of its precipitation during winter, and much of that is brought by the passage of extratropical cyclones and their fronts. During the three consecutive winters of 2011/12 through 2013/14, precipitation over California was all much below average, and most of California experienced either extreme or exceptional drought conditions during much of 2014 [Seager et al., 2014a]. Due to the drought, the statewide water storage in November 2014 was only about 56% of average for that time of the year [Seager et al., 2014a].

Lack of precipitation is not the only cause of the drought. Several studies have suggested that higher than average temperatures during these years also contributed to the dryness [e.g. AghaKouchak et al., 2014; Griffin and Anchukaitis, 2014]. Nevertheless, it is still important to understand the physical drivers behind California precipitation variability, as well as better understand future projections derived from climate model simulations.

In projections of precipitation change in the Coupled Model Intercomparison Project (CMIP) Phase 3 and Phase 5 ensembles of model simulations, precipitation reductions in the subtropics and increases at mid- to high-latitudes tend to be relatively well agreed upon at large scales [Meehl et al., 2007; Collins et al., 2013; Maloney et al., 2014; Seager et al., 2014b]. California lies close to the boundary between these opposing tendencies [Cayan et al., 2008; Pierce et al., 2012], so precipitation change projections require careful scrutiny of uncertainties that can be aided by an understanding of dynamical factors influencing the region. Neelin et al. [2013] note that precipitation change in Central and Southern California constitutes one of the main features of North American end-of-century projections that differs in CMIP5 simulations relative to CMIP3, associated with a change in the storm track precipitation coming onto the coast. This feature is associated with simulated increases in 200 hPa winds in a location that tends to extend the region of strong subtropical jet toward the east, which was postulated to tend to extend the storm track toward the California coast. Chang et al. [2012] and Chang [2013] find a tendency of weakening in measures of storm track or extratropical cyclone activity in hemispheric and aspects of the large-scale North American response, potentially associated with large-scale changes in baroclinicity. Potential changes affecting the California region are closely associated with the regional dynamics where storms approach the coast. Here, we address the connection between measures of extratropical cyclone activity, in particular bandpass-filtered sea level pressure variance, and the changes in precipitation over California, both in interannual variations and in global warming projections.

2. Data and Methods

To obtain the climatological extratropical cyclone activity and precipitation, we have used two analysis data sets to represent observations. Extratropical cyclone activity is calculated based on the National Centers for Environmental Prediction-National Center for Atmospheric Research reanalysis (NNR) data [Kalnay et al. 1996] with a horizontal resolution of 2.5°. Precipitation in California is derived from the Global Precipitation Climatology Project (GPCP, version 2.2) monthly data [Adler et al. 2003], which is a gridded analysis merging satellite observations with gauge measurements. The time periods of both NNR and GPCP data examined are from December 1979 to February 2015, 36 winter seasons (December to February, DJF) in all.

In total 30 CMIP5 models from 18 modeling centers (Table S1) have been examined in this study. These represent all models that have provided 6-hourly data for both the historical and future periods that are currently available from the CMIP5 archives (note that 6-hourly data from FGOALS-s2, examined in some previous studies, have been withdrawn). Extratropical cyclone activity is calculated from 6-hourly data and model precipitation is derived from monthly mean data. Similar to Neelin et al. [2013], we selected 40 winter seasons in both historical runs and Representative Concentration Pathway 8.5 (RCP8.5) simulations to represent the climatology in the 20th Century (1961-2000) and the end of 21st century (2059-2098). The high emission RCP8.5 scenario is analyzed to provide a strong signal. Note that previous studies have suggested that many climate change signals, including projected changes in extratropical cyclone activity, scales roughly linearly with the hemispheric temperature change [e.g., Neelin et al., 2006; Chang, 2013; Tebaldi and Arblaster, 2014]. The winter season extratropical cyclone activity and precipitation changes are defined as the difference between the climatology of historical period and RCP8.5 simulations. All the fields in CMIP5 models are interpolated onto the same 2.5°×2.5°grid before analyses are performed. Models in each ensemble are treated independently, though some of them may have the same structural cores so they may have similar biases [e.g. Knutti et al 2010, 2013]. Historical simulations by FGOALS-g2 fail to capture the relationship between extratropical cyclone activity and precipitation (see discussions below), hence FGOALS-g2 is not included in multi-model ensemble (MME) mean, and all model results are based on 29 CMIP5 models from 17 modeling centers.

Most CMIP5 models only provide 6-hourly data from a single ensemble member. Several models provide data from multiple members, and historical and future experiments from a single ensemble member (usually r1i1p1) are used in the analysis. Since GISS-E2-H and GISS-E2-R only provide 6-hourly historical and future data from different ensemble members, we have used data from different ensemble members (with the same physics) to represent the historical period and RCP8.5 simulations for the two GISS models. CSIRO-Mk3-6-0 has provided the largest number of ensemble members (10), and these 10 members have been analyzed to explore internal climate variability. Results from these 10 members (see discussions below) also confirm that it is appropriate to use different ensemble members to represent historical period and RCP8.5 simulations in our study.

Precipitation in California is defined as the winter season precipitation in the shaded area in Fig.1e (same as the California precipitation box in [Neelin et al. 2013]), which covers about the southern two-thirds of California, where the sign of precipitation projection is uncertain. Extratropical cyclone (or storm track) activity is defined based on temporal variance statistics, band-pass filtered using a 24-hour difference filter [Wallace et al. 1988]:

$$pp = \overline{\{p(t+24hr) - p(t)\}^2} \qquad (1)$$

In equation (1), *p* is sea level pressure (SLP), and *pp* is the 24-hour difference filtered variance of sea level pressure. The overbar corresponds to time averaging for the winter season (DJF). Many previous studies [e.g. Lau, 1978; Wallace et al., 1988; Chang et al., 2002] have suggested that the peaks in this measure lie over geographical locations where cyclone tracks preferentially cross (see also Fig. 1).

3. Results

3.1 Historical period

The climatological distribution of winter extratropical cyclone activity as indicated by *pp* across Eastern North Pacific and North America is shown in Fig. 1a. Maximum activity extends northeastward from Central North Pacific into the Gulf of Alaska and western Canada, and then southeastward across Canada towards the Great Lakes, qualitatively similar to major cyclone tracks that traverse the region [e.g. Hoskins and Hodges 2002]. Our own analyses (not shown) have also shown that this distribution is very similar to the climatological spatial distribution of extratropical cyclone density. Note that the maxima of *pp* are generally located poleward of the mid-latitude maxima in precipitation (not shown here, but see, for example, Fig. 1 of Neelin et al. [2013]). This is because cyclone related precipitation extends far to the equatorward side of cyclone centers along cold and warm fronts [e.g. Chang and Song 2006; Bengtsson et al. 2009].

The multi-model mean *pp* climatology based on historical experiments from CMIP5 models is shown in Fig. 1b. Overall, CMIP5 models are quite successful in simulating the distribution except that the spatial pattern is smoother due to averaging over a large ensemble.

The time series of winter precipitation over the California box (Fig. 1e) based on GPCP data is shown by the blue line in Fig. 2b. There is clearly large year-to-year variability – seasonal precipitation varies from about 1.2 mm day^{-1} in 1990/91 to about 6.4 mm day^{-1} in 1997/98. There is a weak decreasing trend of -0.025 mm day^{-1} year^{-1} between 1979/80 and 2014/15, but this trend is not significant at the 90% level.

To quantify the relationship between California precipitation and extratropical cyclone activity, point-by-point correlation is computed between the California precipitation time series shown in Fig. 2b with the time series of *pp* at each grid box. The resulting correlation map is shown in Fig. 1c. It is clear that California precipitation is strongly correlated with extratropical cyclone activity over Eastern Pacific just to the west of California, with positive correlation reaching over 0.8. This positive correlation is reasonable since most of the precipitation over California is due to passages of extratropical cyclones or their fronts. There is also a weaker but still statistically significant negative correlation spreading across the south coast of Alaska and western Canada, suggesting that the increased cyclone activity over Eastern Pacific that brings more precipitation to California is frequently associated with a south-eastward shift of the East Pacific storm track. Part of this variability is related to the El Niño-Southern Oscillation (ENSO), as previous studies [e.g. Chang et al., 2002] have shown that during El Niño, the Pacific jet is shifted slightly southward and extends eastward towards North America, steering more extratropical cyclones towards California [Held et al., 1989; Straus and Shukla, 1997; Dettinger et al., 1998; Cayan et al., 1999]. However, note that the correlation between winter California precipitation and the Nino-3.4 index is only 0.38 between 1979/80 and 2013/14, indicating that ENSO can only explain part of the relationship between California precipitation and extratropical cyclone activity.

Similar correlation maps have been computed for each of the CMIP5 historical simulations using their own precipitation and extratropical cyclone activity time series, and the average of these correlation maps is shown in Fig. 1d. Overall, CMIP5 models are able to reproduce the main structure of the observed correlation map, with large positive correlations just to the west of California, and weak negative correlations to the north.

Given the strong positive correlation between California precipitation and extratropical cyclone activity just offshore, in both observations and model simulations, an East Pacific box (Fig. 1) is defined covering the region of highest correlations to quantify year-to-year variations of extratropical cyclone activity. Note that results discussed below are not sensitive to the exact definition of the box – we have shifted the box in all directions by 5° as well as changed the size of the box, and very similar results are obtained.

The time series of extratropical cyclone activity averaged over the East Pacific box, based on NNR, is shown by the red line in Fig. 2b. It is clear that this time series is highly correlated with the California precipitation time series. The values of California precipitation and extratropical cyclone activity for each winter are plotted against each other in Fig. 2a. The correlation between the two quantities is about 0.8. Fig. 2b suggests that similar to California precipitation, extratropical cyclone activity also exhibits a small downward trend during this period, but again this trend is not statistically significant. Regardless, the three consecutive winters of low precipitation in the early 2010s (2011/12 through 2013/14) are coincident with three years of low extratropical cyclone activity. Note that the ratio between the two trends shown in Fig. 2b (0.18 mm day^{-1} hPa^{-2}) is consistent with the slope of the regression line between the two quantities based on year-to-year variability (0.17 mm day^{-1} hPa^{-2}; see Fig. 2a).

Scatterplots similar to Fig. 2a have been derived from historical simulations of each of the CMIP5 models, and they are shown in supporting Fig. S1. Twenty nine of the thirty models examined display significant correlation between California precipitation and extratropical cyclone activity averaged over the East Pacific box. The only exception is FGOALS-g2 (bottom right panel in Fig. S1), which differs so clearly from observed behavior that it is excluded from the analyses below.

Considerable model-to-model variability occurs in these historical relationships (Fig. S1). The correlation varies between a high of 0.93 for CCSM4 to a low of 0.44 for GFDL-ESM2G. The multi-model mean correlation is 0.71. The slope of the regression line also varies from 0.07 mm day^{-1} hPa^{-2} for GFDL-ESM2G to 0.24 mm day^{-1} hPa^{-2} for MIROC5, with the multi-model mean slope being 0.16 mm day^{-1} hPa^{-2}, consistent to the observed slope (0.17 mm day^{-1} hPa^{-2}) discussed above. To see how much of the variability might be due to internal climate variability rather than to model uncertainties [e.g. Hawkins and Sutton, 2011; Deser et al. 2012], similar analyses have been performed on 10 ensemble members from CSIRO-Mk3.6.0 which use the same model forced by the same climate forcings. Scatterplots from these 10 simulations are shown in supporting Fig. S2. Among these 10 simulations, the correlation between California precipitation and East Pacific extratropical cyclone activity varies from 0.72 and 0.85, while the slope of the regression line varies from 0.16 to 0.24 mm day^{-1} hPa^{-2}. Comparing results shown in Figs. S1 and S2, while climate variability can give rise to significant variability in the relationship between California precipitation and extratropical cyclone activity, it is unlikely that internal climate variability can explain all the model-to-model differences. Overall, most models successfully simulate a tight relationship between California precipitation and East Pacific extratropical cyclone activity.

3.2 Future projections

CMIP5 multi-model ensemble mean projected change in precipitation is shown in Fig. 3a, and model agreement is shown in Fig. 3b. Consistent with Neelin et al. [2013], increased precipitation is projected over much of California, including much of the box shown in Fig. 1e. Overall, a majority of the models project precipitation increase over most of the region. Nevertheless, there are significant model-to-model differences in the magnitude of the projected change, with the California box averaged precipitation projected to change by nearly -1 mm day^{-1} to a bit over +2 mm day^{-1} (see Fig. 4a).

Projected change in extratropical cyclone activity is shown in Fig. 3c. On average, CMIP5 models project a small but statistically significant increase in extratropical cyclone activity over Eastern Pacific, and a majority of the models project increase over much of the East Pacific box (Fig. 3d), especially over the northwestern part of the box. Averaged over the box, the projections range from a bit less than -4 hPa^2 to more than +10 hPa^2. The models also project significant decrease to the north of this region, consistent with the results of Chang et al. [2012]

that cyclone tracks over the East Pacific just off the North America coast are projected to shift southward by CMIP5 models.

In Fig. 4a, each model's projected precipitation change over the California box is plotted against its projected change in extratropical cyclone activity averaged over the East Pacific box. There is clearly high correlation between these two projected changes, with the inter-model correlation being 0.85. The slope of the regression between these two quantities (0.18 mm day^{-1} hPa^{-2}) is also close to the ensemble mean slope of the year-to-year variability discussed above (0.16 mm day^{-1} hPa^{-2}). Among the 29 models, the two MRI models project the largest increase in both precipitation and extratropical cyclone activity and are apparent outliers. Nevertheless, even if we remove results from these two models, the correlation between the other 27 models is still quite high (0.73), with a regressed slope of about 0.15 mm day^{-1} hPa^{-2}, again close to the multi-model mean regressed slope based on the historical period.

Given the strong physical and statistical relationships between California precipitation and East Pacific extratropical cyclone activity, we hypothesize that model projected change in California precipitation can be "predicted" by model projected change in extratropical cyclone activity. To predict precipitation projection based on projected change in extratropical cyclone activity, for each model, its projected change in extratropical cyclone activity is multiplied by the regression coefficient between California precipitation and extratropical cyclone activity found in its historical simulation. For example, MRI-CGCM3 projects an increase in extratropical cyclone activity of about 10 hPa^2 over the East Pacific box (Fig. 4a). Based on its historical simulation, the regression slope between California precipitation and East Pacific extratropical cyclone activity is 0.206 mm day^{-1} hPa^{-2} (see Fig. S1). These two quantities are then multiplied together to represent the model's predicted change in California precipitation based on its projected change in extratropical cyclone activity, and the result comes out to be about 2.1 mm day^{-1}. This "predicted" quantity is then plotted against the model's actual projected change in California precipitation in Fig. 4b. This procedure is repeated for all models, and the resulting plot is shown in Fig. 4b.

Fig. 4b shows that there is a tight relationship between each model's precipitation projection and the prediction based on its extratropical cyclone projection. The correlation between these two quantities is about 0.79, and the slope of the relationship (0.97) is close to 1. Even if we remove the results of the two MRI models, the correlation remains quite high (0.61) and the slope, while smaller, is not statistically different from the slope of the regression that includes the two models.

To assess how much of the model-to-model differences shown in Fig. 4 could be due to climate variability rather than model (or response) uncertainties, projections of changes in precipitation and extratropical cyclone activity based on the 10 ensemble members of CSIRO-Mk3.6.0 have been examined, and analyses similar to those presented in Fig. 4 have been conducted on the 10 ensemble members (supporting Fig. S3). Results from these 10 members from the same model under the same forcing show substantial spread, covering about 40% of the spread shown in Fig. 4. Member-to-member differences in projected changes in California precipitation are also well correlated with (and well predicted by) member-to-member differences in projected changes in East Pacific extratropical cyclone activity. Examining the anomalies of each member relative to the ensemble mean, no significant correlation is found between each member's precipitation (or extratropical cyclone activity) anomaly during the historical period with its anomaly in the future, i.e., as expected, internal variability has little memory across the intervening half-century. Comparing historical simulation and future prediction from different ensemble members, these combinations also lie along the same regression lines as those from the same ensemble member (see Fig. S3). This justifies using results from different ensemble members for the GISS models, for which historical and future results from the same ensemble member are not available.

4. Summary and Discussions

California winter precipitation is shown to be strongly modulated by variability and change in extratropical cyclone activity over East Pacific just off the California coast in reanalysis data and CMIP5 simulations. Analyses of interannual variability in California precipitation and East Pacific extratropical cyclone activity reveal that winter-to-winter variations in precipitation are strongly correlated with variations in extratropical cyclone activity. This is not surprising since much of California's precipitation comes from passage of extratropical cyclones and their frontal systems. The recent severe drought in California is coincident with winters in which East Pacific extratropical cyclone activity is much reduced. Both California precipitation and East Pacific cyclone activity display weak decreasing trends between 1979/80 to 2014/15, but neither trend is statistically significant.

Examination of climate projections made by 29 CMIP5 models under the high emission RCP8.5 pathway suggests a small ensemble mean increase in precipitation over much of California, consistent with a small projected increase in East Pacific extratropical cyclone activity. Nevertheless, consistent with previous studies, this region lies close to the transition zone between projected mid-latitude increase and subtropical decrease in precipitation, thus there is significant model-to-model variability in the projected change in precipitation, with some models projecting future decrease while a majority of the models (23 out of 29) project increase. Our analyses show that model-to-model differences in projected change in California precipitation is highly correlated with model-to-model differences in projected change in East Pacific extratropical cyclone activity. In fact, using the relationship between interannual cyclone activity and precipitation variability from the historical period, one can accurately "predict" each model's projected California precipitation change using its projected change in East Pacific extratropical cyclone activity. All these demonstrate that variability and change in California precipitation is highly modulated by those in East Pacific extratropical cyclone activity.

Neelin et al. [2013] showed that model-to-model differences in projected change in California precipitation are highly correlated with those of the upper level jet stream, and they hypothesized that this correlation represents the effect of the jet steering storm tracks (or extratropical cyclones) towards the California coast. In this study, we have directly demonstrated this physical link between storm tracks and California precipitation. Comparing our results to those of Neelin et al. [2013], the relationship between projected changes in California precipitation and East Pacific extratropical cyclone activity is apparently stronger than the relationship between precipitation and upper level jet (compare our Fig. 4 to their Figs. 7 and 10), which is not surprising given the more direct physical linkage between extratropical cyclones and precipitation.

Our analyses of results taken from 10 ensemble members of CSIRO-Mk3.6.0 suggest that part of the model-to-model differences found in this study may be due to internal climate variability, but uncertainties in model response likely still account for much of this spread. The physical mechanisms that give rise to these differences in model response in extratropical cyclone activity and its associated precipitation thus provide a research target of leading importance for California water resources.

Acknowledgments. The authors would like to thank the Earth System Grid and the climate modelling centers for making available the CMIP5 model data. The Stony Brook authors are supported by NSF grant AGS-1261311, and JDN by NSF grant AGS-1102838.

References

Adler, R.F., G.J. Huffman, A. Chang, R. Ferraro, P. Xie, J. Janowiak, B. Rudolf, U. Schneider, S. Curtis, D. Bolvin, A. Gruber, J. Susskind, and P. Arkin (2003), The Version 2 Global Precipitation Climatology Project (GPCP) Monthly Precipitation Analysis (1979-Present), *J. Hydrometeor.*, *4*, 1147-1167.

AghaKouchak, A., L. Cheng, O. Mazdiyasni, and A. Farahmand (2015), Global warming and changes in risk of concurrent climate extremes: Insights from the 2014 California drought. *Geophys. Res. Lett.*, *in press*, doi: 10.1002/2014GL062308.

Bengtsson, L., K. I. Hodges, and N. Keenlyside (2009), Will extratropical storms intensify in a warmer climate? *J. Climate*, *22*, 2276-2301.

Cayan, D. R., K. T. Redmond, and L. G. Riddle (1999), ENSO and hydrologic extremes in the Western United States. *J. Climate*, **12**, 2881-2893.

Cayan, D. R., E. P. Mauer, M. D. Dettinger, M. Tyree, and K. Hayhoe (2008), Climate change scenarios for the California region. *Climatic Change*, **87**, S21-S42.

Chang, E. K. M. (2013), CMIP5 projection of significant reduction in extratropical cyclone activity over North America, *J. Clim.*, *26*, 9903-9922.

Chang, E. K. M., and S. Song (2006), The seasonal cycles in the distribution of precipitation around cyclones in the Western North Pacific and Atlantic, *J. Atmos. Sci.*, *63*, 815-839.

Chang, E. K. M., S. Lee, and K. L. Swanson (2002), Storm track dynamics, *J. Clim.*, *15*, 2163-2183.

Chang, E. K. M., Y. Guo, and X. Xia (2012), CMIP5 multimodel ensemble projection of storm track change under global warming. *J. Geophys. Res.*, *117*, D23118.

Collins, M., R. Knutti, J. Arblaster, J.-L. Dufresne, T. Fichefet, P. Friedlingstein, X. Gao, W.J. Gutowski, T. Johns, G. Krinner, M. Shongwe, C. Tebaldi, A.J. Weaver and M. Wehner, (2013), Long-term Climate Change: Projections, Commitments and Irreversibility. In: Climate Change 2013: The Physical Science Basis. Contribution of Working Group I to the Fifth Assessment Report of the Intergovernmental Panel on Climate Change [Stocker, T.F., D. Qin, G.-K. Plattner, M. Tignor, S.K. Allen, J. Boschung, A. Nauels, Y. Xia, V. Bex and P.M. Midgley (eds.)]. Cambridge University Press, Cambridge, United Kingdom and New York, NY, USA.

Deser, C., A. Phillips, V. Bourdette, and H. Teng (2012), Uncertainty in climate change projections: the role of internal variability, *Clim. Dyn.*, *38*, 527-546.

Dettinger, M. D., D. R. Cayan, H. F. Diaz, and D. M. Meko (1998), North-south precipitation patterns in Western North America on interannual-to-decadal timescales. *J. Climate*, **11**, 3095-3111.

Griffin, D., and K.J. Anchukaitis (2015), How unusual is the 2012-2014 California drought? *Geophys. Res. Lett.*, *in press*, doi:10.1002/2014GL062433.

Hawkins, E., and R. Sutton (2011), The potential to narrow uncertainty in projections of regional precipitation change, *Clim. Dyn.*, *37*, 407-418.

Held, I. M., S. W. Lyons, and S. Nigam (1989), Transients and the extratropical response to El Niño. *J. Atmos. Sci., 46*, 163-174.

Hoskins, B. J., and K. I. Hodges (2002), New perspectives on the Northern Hemisphere winter storm tracks, *J. Atmos. Sci., 59*, 1041-1061.

Kalnay, E., and coauthors (1996), The NCEP/NCAR 40-year reanalysis project, *Bull. Amer. Meteor. Soc., 77*, 437-470.

Knutti, R., R. Furrer, C. Tebaldi, J. Cermak, and G. A. Meehl (2010), Challenges in combining projections from multiple climate models. *J. Clim., 23*, 2739-2758.

Knutti, R., D. Masson, and A. Gettelman (2013), Climate model genealogy: Generation CMIP5 and how we got there, *Geophys. Res. Lett., 40*, 1194-1199.

Lau, N.-C. (1978), On the three-dimensional structure of the observed transient eddy statistics of the Northern Hemisphere wintertime circulation. *J. Atmos. Sci., 35*, 1900-1923.

Maloney, E. D. and coauthors (2014), North American Climate in CMIP5 Experiments. Part III: Assessment of 21st Century Projections, *J. Climate*, 27, 2230-2270, doi:10.1175/JCLI-D-13-00273.1.

Meehl, G., T. F. Stocker, W. Collins, and coauthors (2007), Global climate projections. Climate Change 2007: The Physical Science Basis. Contribution of Working Group I to the Fourth Assessment Report of the Intergovernmental Panel on Climate Change, S. Solomon, D. Qin, and M. Manning, Eds., Cambridge University Press, Cambridge and New York, 996pp.

Neelin, J. D., M. Munnich, H. Su, J. E. Meyerson, and C. E. Holloway (2006), Tropical drying trends in global warming models and observations, *Proc. Natl. Acad. Sci., 103*, 6110-6115.

Neelin, J. D., B. Langenbrunner, J. E. Meyerson, A. Hall, and N. Berg (2013), California winter precipitation change under global warming in the Coupled Model Intercomparison Project Phase 5 ensemble, *J. Clim., 26*, 6238-6256.

Pierce, D. W., T. Das, D. R. Cayan, E. P. Mauer, N. L. Miller, Y. Bao, M. Kanamitsu, K. Yoshimura, M. A. Snyder, L. C. Sloan, G. Franco, and M. Tyree (2012), Probabilistic estimates of future changes in California temperature and precipitation using statistical and dynamical downscaling, *Climate. Dyn*., doi: 10.1007/s00382-012-1337-9.

Seager, R., M. Hoerling, S. Schubert, H. Wang, B. Lyon, A. Kumar, J. Nakamura, and N. Henderson (2014a), Causes and predictability of the 2011-14 California drought. DTF/NIDIS Assessment Report, doi:10.7289/V58K771F

Seager, R., J. D. Neelin, I. Simpson, H. Liu, N. Henderson, T. Shaw, Y. Kushnir, M. Ting, and B. Cook (2014b), Dynamical and thermodynamical causes of large-scale changes in the hydrological cycle over North America in response to global warming, *J. Climate*, 27, 7921–7948, doi:10.1175/JCLI-D-14-00153.1.

Straus, D. M., and J. Shukla (1997), Variations of midlatitude transient dynamics associated with ENSO. *J. Atmos. Sci*., *54*, 777-790.

Tebaldi, C., and J. M. Arblaster (2014), Pattern scaling: Its strengths and limitations, and an update on the latest model simulations. *Climatic Change*, *122*, 459-471, doi:10.1007/s10584-013-10.

Wallace, J. M., G.-H. Lim, and M. L. Blackmon (1988), Relationship between cyclone tracks, anticyclone tracks and baroclinic waveguides, *J. Atmos. Sci*., *45*, 439-462.

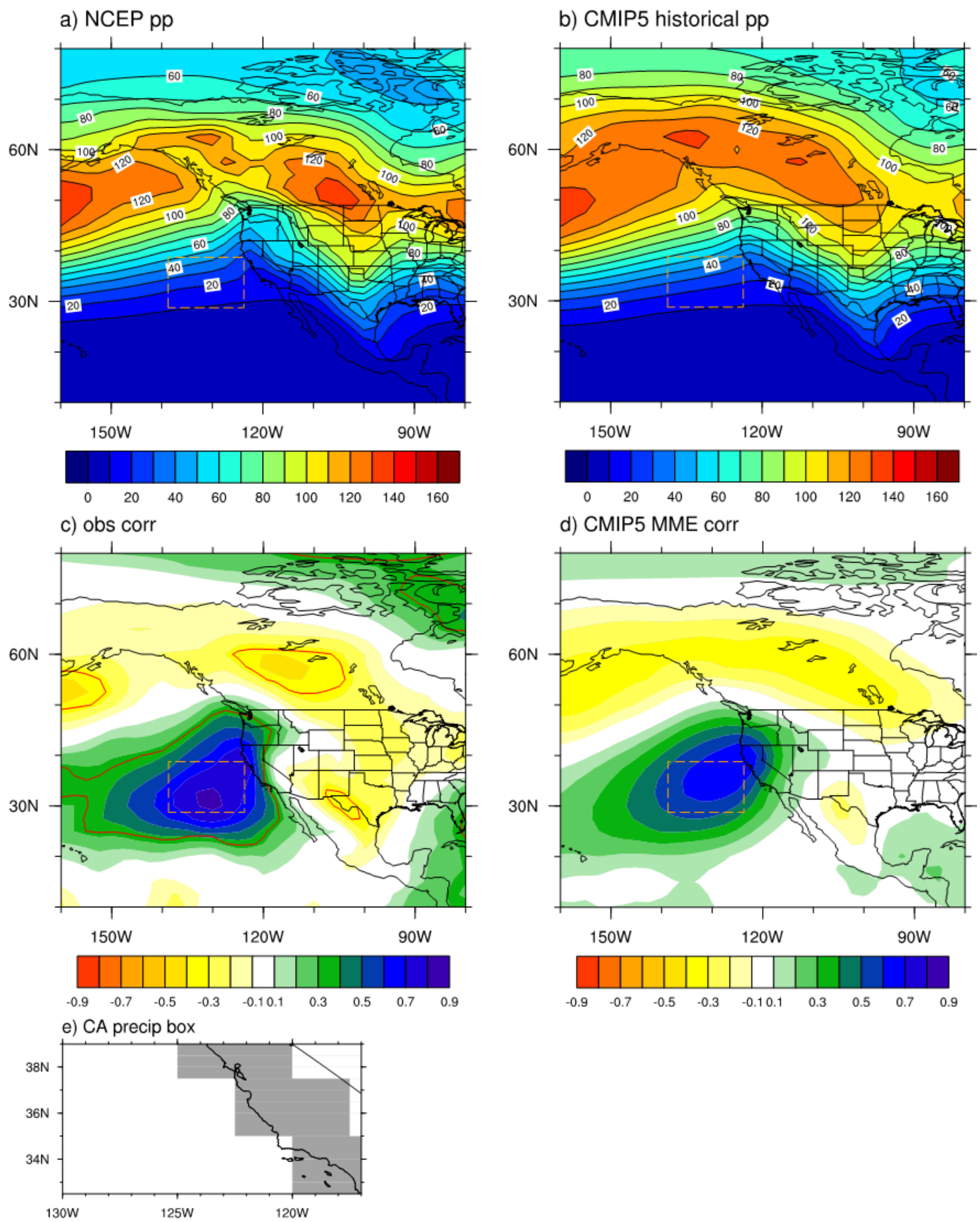

Fig. 1: a) NCEP DJF bandpass-filtered SLP variance, *pp*, climatology from 1979/80 to 2014/15. b) CMIP5 29-model ensemble mean historical pp climatology from 1961 to 2000. c) Correlation map of GPCP DJF precipitation averaged over the CA precipitation box and NCEP DJF pp at each grid point from 1979/80 to 2014/15. The red contour shows the correlation is at 95% statistical significant level. d) Mean of correlation maps of DJF precipitation in CA box and DJF pp from 1961 to 2000. e) The shaded region is used to calculate precipitation in CA. The dashed box shown in panels a-d is the box used to compute East Pacific extratropical cyclone activity.

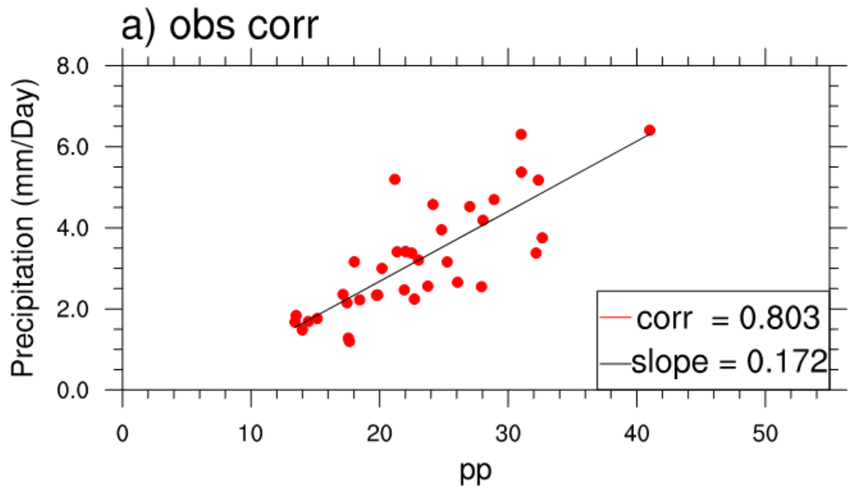

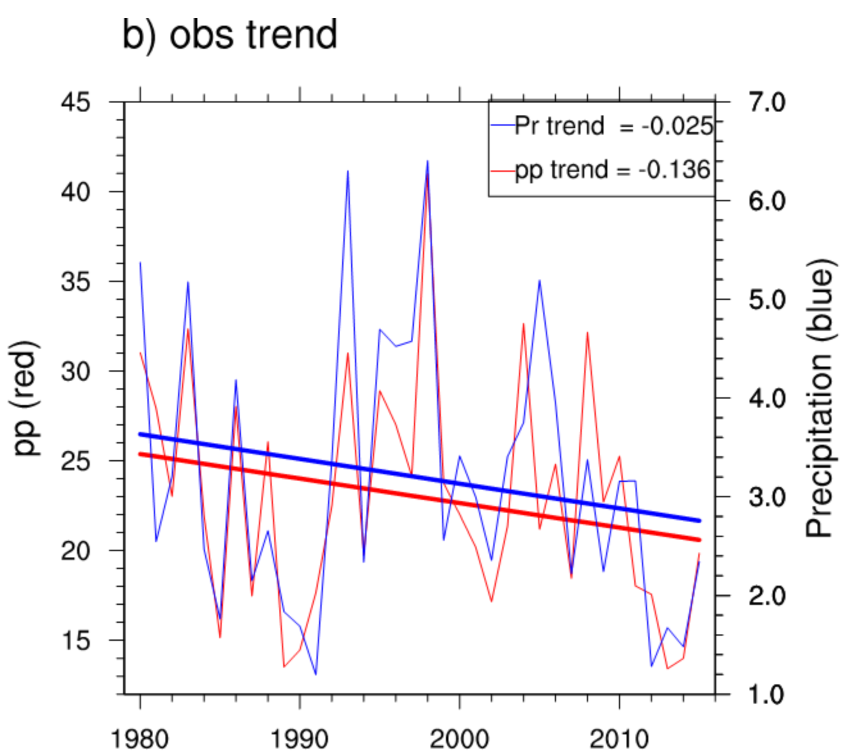

Fig. 2: a) Scatterplot of NCEP reanalysis *pp* (hPa^2) in the East Pacific extratropical cyclone activity box (see Fig. 1c) vs. GPCP precipitation (mm/day) in California region (see Fig. 1e) during DJF from 1979/80 to 2014/15. b) The time series of the two quantities. Precipitation is in blue color and has a decreasing trend of -0.025 mm/day/year, and pp is in red color and has a decreasing trend of -0.136 hPa^2/year. Neither precipitation nor pp shows a statistically significant trend.

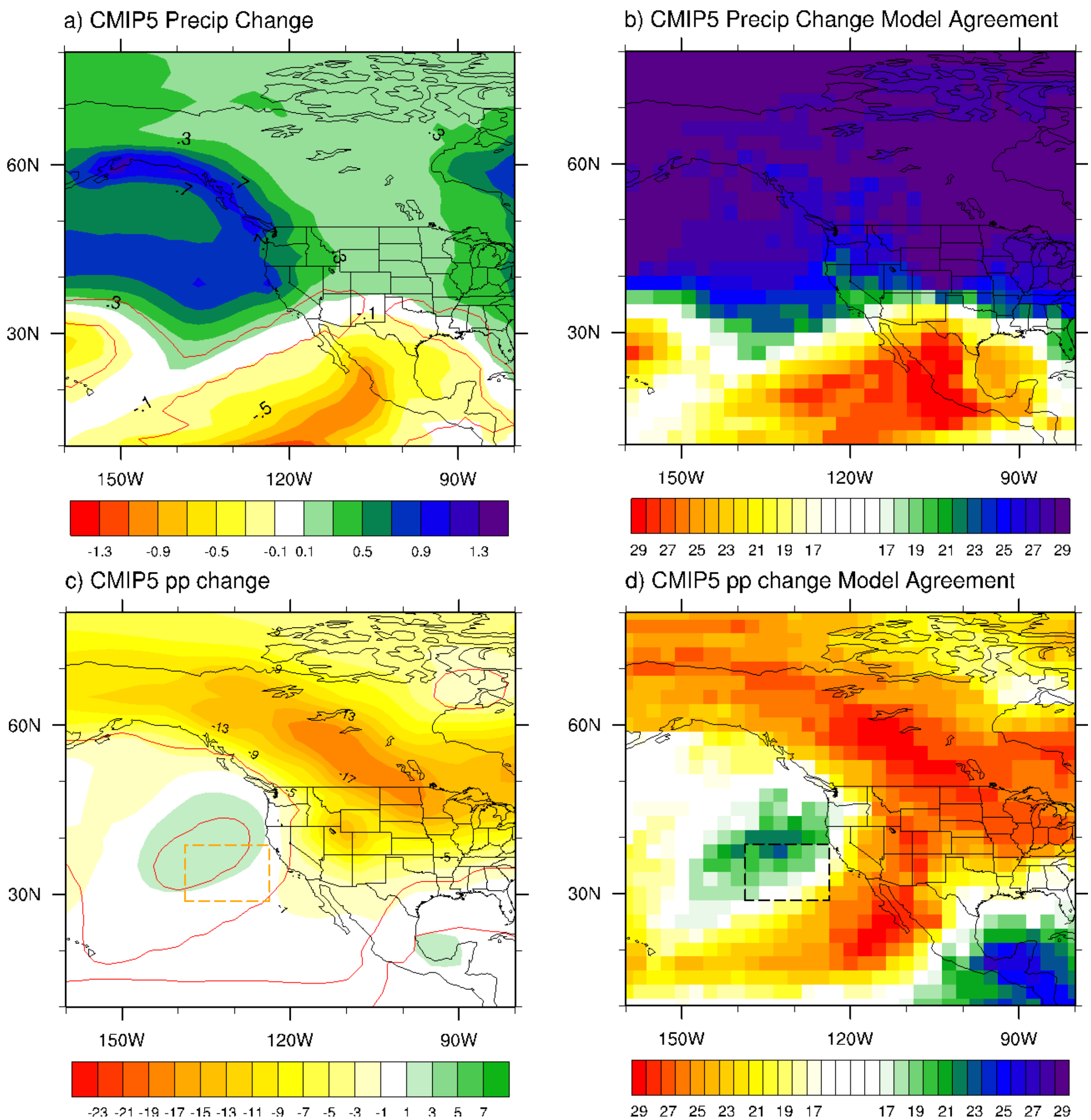

Fig. 3: a) CMIP5 multi-model ensemble mean projection of DJF precipitation (mm/day) change from 1961-2000 to 2059-2098. The red line shows the 95% inter-model statistical significant level based on a student's t-test. b) Similar to a) but showing the model agreement. The warm colors show the number of models that project precipitation decrease and cold colors show the number of models that project precipitation increase. c)-d) Same as a)-b) but for projected pp (hPa^2) change.

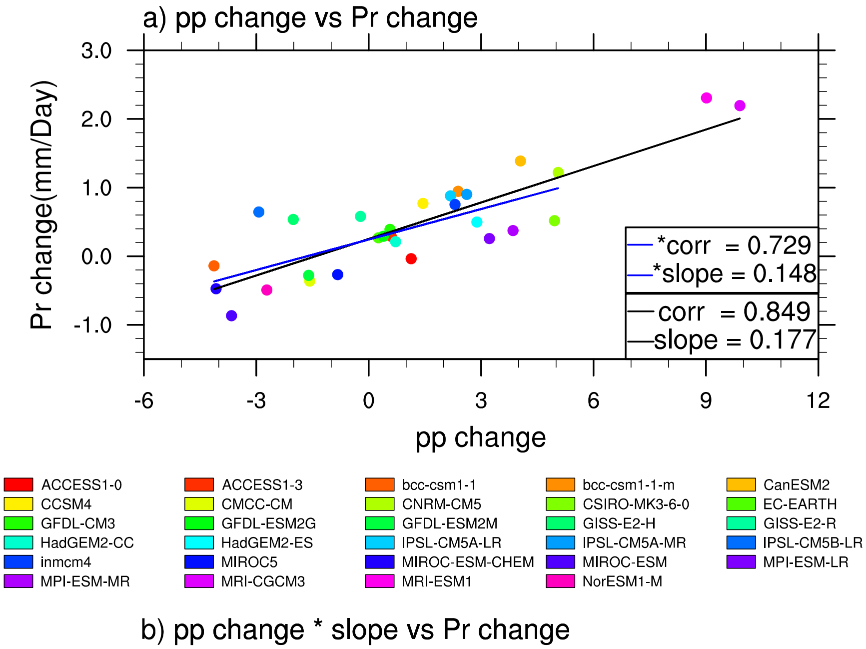

Fig. 4: a) Scatterplot showing CMIP5 East-Pacific *pp* (hPa^2) cyclone activity index change vs precipitation (mm/day) change for each model. Both pp and precipitation change are the difference between RCP8.5 run from 2059-2098 DJF and historical run from 1961-2000 DJF. Black line shows the regression line (and correlation, corr, and slope values) corresponding to all CMIP5 models. Blue line shows the regression line (and *corr and *slope values) corresponding to when MRI-CGCM3 and MRI-ESM1 are excluded. b) Ordinate shows model projected California DJF precipitation change (2059-2098 minus 1961-2000), and abscissa shows the DJF pp change (2059-2098 minus 1961-2000) multiplied by slope for precipitation change per unit pp change derived from historical runs in each model (see Supplemental Fig. S1). MME Mean (black) point shows the multi-model ensemble mean of the value in x-axis and y-axis. Black line, corr and slope values correspond to all CMIP5 models. Blue line and *corr and *slope values correspond to when MRI-CGCM3 and MRI-ESM1 are excluded.